12

Theory and Applications of Metamaterial Covers

Mehdi Veysi, Amir Jafargholi and Manouchehr Kamyab
E.E. Dept. K. N. Toosi University of Technology, Tehran, Iran

1. Introduction

Metamaterial covers exhibit inimitable electromagnetic properties which make them popular in antenna engineering. Two important features of metamaterial covers are: (1) increasing of the transmission rate and (2) control of the direction of the transmission which enable one to design directive antennas. In this chapter, the possibility of increasing both bandwidth and directivity of the printed patch antenna using metamaterial covers is examined. The printed patch antennas are a class of low-profile antennas, which are conformable to planar surfaces, simple and inexpensive to manufacture using printed-circuit technology.

Furthermore, novel polarization-dependent metamaterial (PDMTM) covers, whose transmission phases for two principal polarizations are different, are presented (Veysi et al., 2011). A full-wave Finite Difference Time Domain (FDTD) numerical technique is adopted for the simulations. A schematic of the metamaterial cover with square holes is shown in Fig. 1. It consists of two planar layers with similar square lattices. It was demonstrated in (Pendry et al., 1996; Tsao & Chern, 2006) that in the frequency range, where the wavelength is very large compared to the period of the metamaterial cover, this structure acts as a homogenous medium. The equivalent refractive index of this medium, in the microwave domain, is given by:

$$n_{eff} = \sqrt{1 - \left(f_P / f \right)^2} \tag{1}$$

where f_P denotes the plasma frequency and f denotes the operating frequency. If the operating frequency is selected slightly larger than the natural plasma frequency of the metamaterial cover, the equivalent refractive index will be extremely low. Consequently, the transmission phase at the plasma frequency is extremely low.

The ultra refraction phenomena, in which the transmitted rays are parallel to each other, can be expected where the transmission coefficient reaches its maximum value. In other words, the zero transmission phase occurs at the same frequencies where the magnitude of the transmission coefficient becomes maximum. Hence, it acts similar to an equally phase surface at its plasma frequency. It is evident from Eq.1, that the equivalent refractive index and thus the antenna directivity are very sensitive to the frequency.

As a starting point, we consider a two-layer metallic grid placed on top of the patch antenna backed by a ground plane. The simulations have been carried out to examine the

transmission characteristic of the metamaterial cover, without the ground plane and without the antenna, using FDTD code developed by the authors.

Fig. 2 shows an effective unit cell model of the metamaterial cover which takes into account the image effect of the ground plane. This unit cell is a convenient method of computing of the transmission coefficient of a two layer metamaterial cover placed on top of the patch antenna backed by a ground plane. Here, Perfect Match Layers (PMLs) are applied to realize a medium with no reflection. The normalization in the code consists of choosing the peak magnitude of the transmission coefficient to be unity. Therefore, the magnitude of the transmitted field from the metamaterial cover has been normalized to that without the metamaterial cover. We have used the same methodology applied in the measurements (Enoch et al., 2002). The periodic boundary conditions (PBCs) have been also applied to model an infinite periodic replication. Since an infinite periodic structure has been simulated, the peak magnitude of the transmission coefficient is unity, unlike the results obtained in the measurements (Enoch et al., 2002).

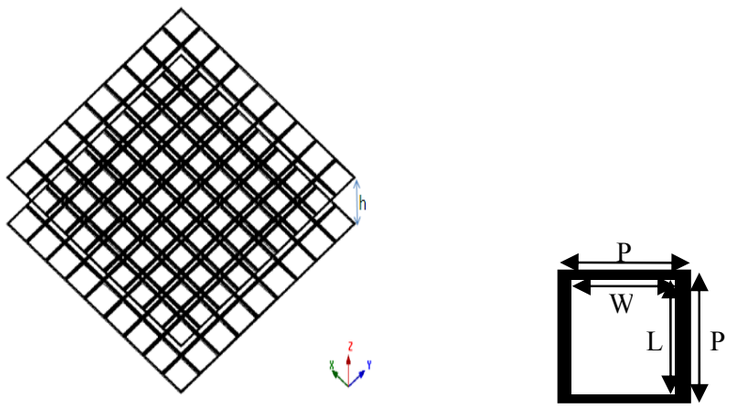

Fig. 1. Schematic view of two layer metamaterial cover together with its unit cell (Veysi et al., 2011).

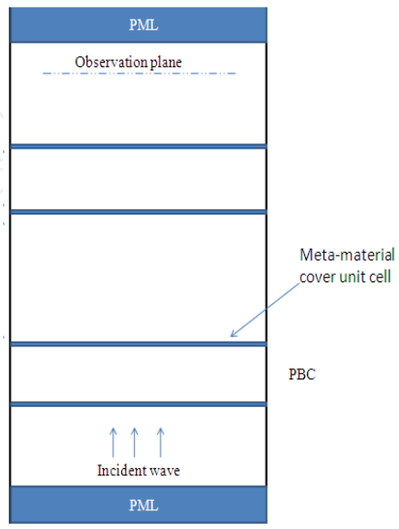

Fig. 2. FDTD model for metamaterial cover analysis (Veysi et al., 2011).

2. Directivity and bandwidth enhancement of proximity-coupled microstrip antenna

Directive patch antennas are very popular in electromagnetic community. Their attractive features, such as low profile, light weight, low cost and compatibility with Microwave Monolithic Integrated Circuits (MMICs), do not exist in other antennas.

Two distinctive types of directive antennas are parabolic antennas and large array antennas. Bulk and curved surface of parabolic antennas limits their use in many commercial applications. Also, complex feeding mechanism and loss in the feeding network are two major disadvantages associated with microstrip array antennas.

One solution to these problems is to use metamaterial cover over the patch antenna (Alu et al., 2006; Xu et al., 2008; Zhu et al., 2005; Huang et al., 2009). One of the first works was done by B. Temelkuaran in 2000, (Temelkuaran et al., 2000). In 2002, S. Enoch proposed a kind of metamaterial for directive emission, (Enoch et al., 2002). Another problem associated with microstrip antennas is their narrow bandwidth. The previous works so far (Xu et al., 2008; Zhu et al., 2005; Huang et al., 2009) have dealt only with the enhancement of the antenna directivity using metamaterial cover, but the effect of this cover on the antenna input impedance has not been investigated.

Recently, a new metamaterial cover has been proposed to enhance both the antenna bandwidth and directivity, (Ju et al., 2009). But, its directivity is significantly lower compared to the primary metamaterial cover, (Xu et al., 2008; Zhu et al., 2005; Huang et al., 2009).

In this section, it is demonstrated that both the impedance and directivity bandwidths of the proximity-coupled patch antenna can be enhanced using the metamaterial cover. It is known that proximity-coupled patch antennas are sensitive to the transverse feed point location. In the case at hand, a parasitic microstrip line has been used on the opposite side of the feed line to mitigate this drawback (Jafargholi et al., 2011). The dimensions of the analyzed metamaterial cover are:

$$P=0.41\lambda_{6GHz},\ t=0.01\ \lambda_{6GHz},\ L=0.31\lambda_{6GHz},\ h=0.49\lambda_{6GHz} \tag{2}$$

Where λ_{6GHz} (50mm) denotes the free space wavelength at 6GHz, P is the periodicity, t is the thickness of the metallic grids, L is the edge of the square holes and h is the distance between the two sheets which is the same as the distance between the patch antenna and the first sheet.

In the FDTD simulations, a uniform $0.01\lambda_{6GHz}$ grid size is used. The resulting transmission curve is plotted in Fig.3. As can be seen, this structure has three microwave plasma frequencies at about 5GHz, 5.81GHz and 8.1GHz which make it suitable for the antenna applications. When the aforementioned metamaterial cover is placed over the conventional proximity-coupled patch antenna, the final metamaterial antenna can be approximated by a homogenous medium terminated in a ground plane.

This approximation is similar to that used for the transmission coefficient calculations. It is a simple matter to obtain the surface impedance of this grounded slab as a function of metamaterial parameters. A surface impedance of the grounded slab of thickness h is:

$$Z_s = j\eta \tan(2\pi h / \lambda) \tag{3}$$

where η and λ are the wave impedance and wavelength in the slab, respectively. For the extremely low values of ε_{eff}, the surface impedance is inductive. In addition, the inductive reactance is $X_l=j\omega L$.

For equivalence we can equate them, leading to the following equation:

$$j\omega L = j\eta \tan(2\pi h / \lambda) \tag{4}$$

Since ε_{eff}<<1 we can apply the small-angle approximation, so that above equation then becomes $L=\mu_0 h$. Consequently, the operation mechanism of this metamaterial based cover can be explained using this equivalent inductance.

In addition, coupling between the feed line and the patch antenna is totally capacitive. And thus, one can expect another resonant frequency due to the reactive cancellation between the capacitive feeding structure and the inductive metamaterial cover. Consequently, an appropriate selection of the coupling capacitor value can result in a broadband operation. To this aim, the metamaterial cover described above is placed over the conventional proximity-coupled patch antenna.

A schematic of proposed metamaterial patch antenna is shown in Fig. 4. In general, the two dielectrics can be of different thicknesses and relative permittivity, but here both dielectrics are 0.762mm Duroid with, ε_r= 2.2. For the case discussed here, the patch of the antenna is rectangular with 12.45mm width and 16mm length.

The distance between the main microstrip line and the parasitic line is also 7mm. Each metamaterial cover composed of 9×9 unit cells, as shown in Fig.4. Consequently, the total size of the dielectric substrate and the metamaterial cover is 184.5mm×184.5mm. Furthermore, the working frequency of the conventional patch antenna is selected at 5.9GHz.

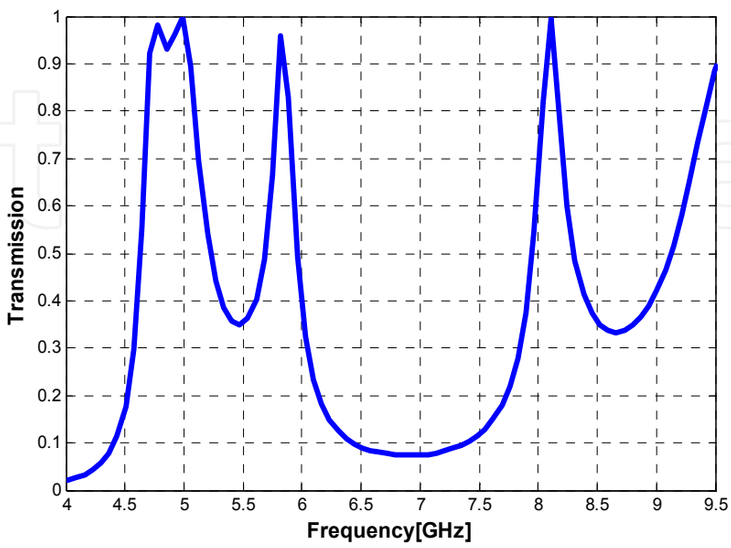

Fig. 3. FDTD simulated transmission of metamaterial cover.

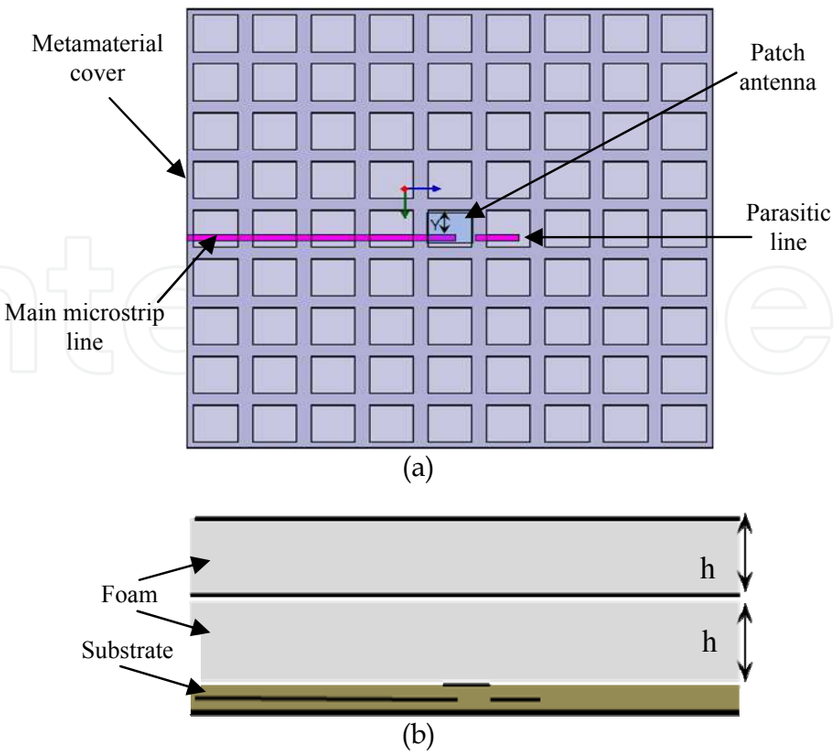

Fig. 4. Geometry of a metamaterial proximity-coupled patch antenna, (a) top view and (b) cross view.

Reflection coefficient of the proposed metamaterial patch antenna has been simulated and was compared to the one obtained for the conventional proximity-coupled patch antenna in Fig. 5. As revealed in the figure, the antenna return loss is significantly improved compared to the reference patch antenna without the metamaterial cover.

The impedance bandwidth of the patch antenna is increased from 2.9% to 5.23% (ranging from 5.649GHz to 5.952GHz). Using the usual formulas mentioned in (Garg et al., 2001), the conventional proximity-coupled patch antenna discussed here has a TM_{01} mode resonant frequency of approximately 5.9GHz. The second resonant frequency of the metamaterial patch antenna is obviously due to the TM_{01} mode of the conventional patch antenna. (See Fig.5)

Since the metamaterial superstrate disturbs the current distribution of the TM_{01} mode, this resonant frequency slightly shifts down to a lower frequency. An interested reader is recommended to refer to (Zhong et al., 1994) for more details. The first resonant frequency is the result of reactive cancellation between the capacitive feeding structure and the inductive metamaterial cover.

On the other hand, the first resonant frequency is close to the second resonant frequency, which results in broadband operation. The simulation results of Fig. 5 are in good agreement with the theoretical predictions discussed above, which serve to justify the approximations used to model the metamaterial patch antenna as a grounded homogenous medium.

It is necessary to mention that the parasitic line section, used on the opposite side of the feed line, stabilizes the antenna performance at its resonant frequency at the expense of an additional resonance frequency at about 6.24GHz (Jafargholi et al., 2011). By using the metamaterial cover over the patch antenna, the antenna radiation patterns in E- and H-planes are concentrated in a direction perpendicular to the patch antenna (θ=0).

The simulated broadside directivity versus frequency is shown in Fig. 6. As can be seen, the maximum directivity of the patch antenna is increased from 6.25dB to16.16dB using metamaterial cover. The 3dB directivity bandwidth of the metamaterial antenna is also between 5.685GHz and 5.91GHz, or 3.88%.

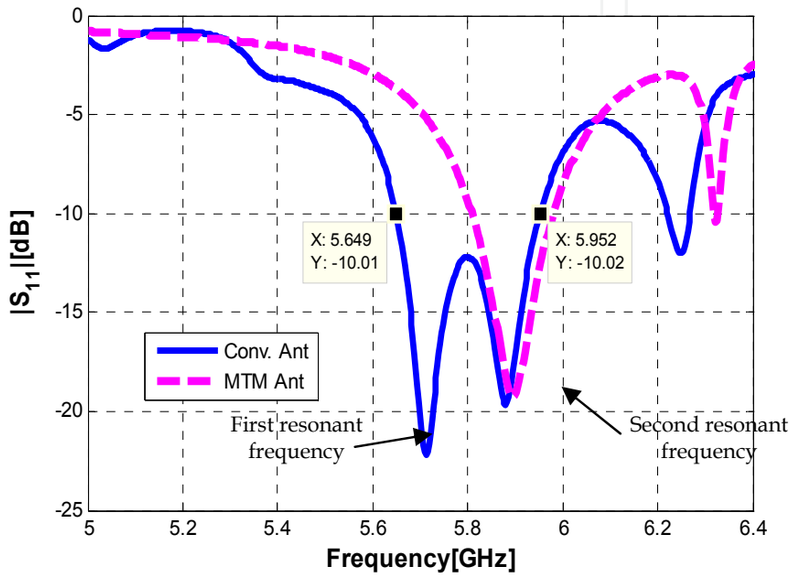

Fig. 5. Simulated reflection coefficient versus frequency.

The antenna radiation patterns within its bandwidth are also investigated. The E-plane and H-plane patterns of the metamaterial patch antenna at three frequencies (5.7GHz, 5.8GHz and 5.9GHz) have been simulated and were compared to the one obtained for the conventional antenna, at 5.9GHz, in Fig. 7.

Although the radiation pattern of the metamaterial antenna changes a bit at each frequency, the main lobe of the metamaterial antenna at all frequencies (ranging from 5.65 to 5.95GHz) is in the broadside direction and maximum directivity is reasonably good. The variation of the radiation pattern is mainly attributed to the nature of metamaterial cover.

The maximum directivities of the metamaterial antenna at 5.7GHz and 5.9GHz are 13.24dB and 14dB, respectively. The maximum directivity of an aperture antenna is calculated by $D_{max}=4\pi A/\lambda^2$. In the present case, the area of the aperture is A=and $\lambda=c_0/f_0$= 51.724mm, so that maximum directivity then becomes D_{max}= 22dB.

The maximum directivity of the metamaterial patch antenna, occurring at 5.81GHz, (16.16dB) has approached the maximal directivity obtained, theoretically, with the same aperture size.

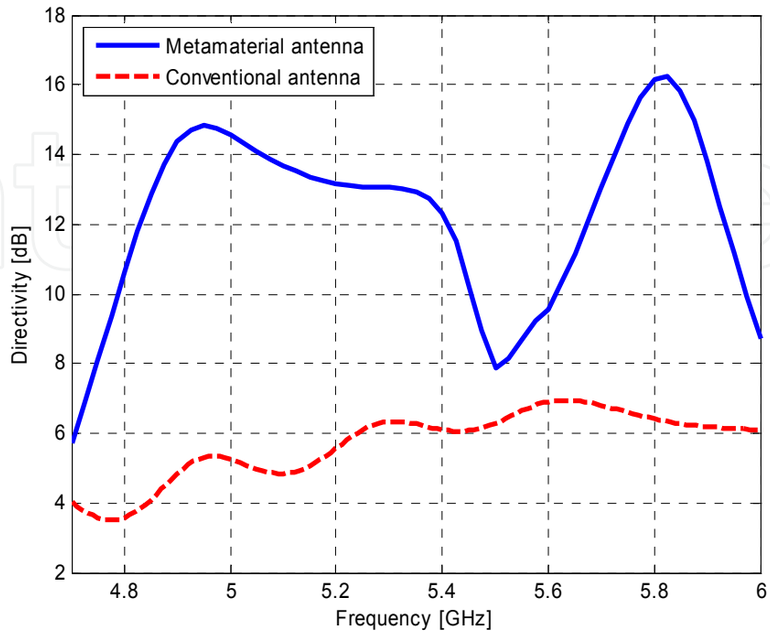

Fig. 6. Simulated broadside directivity versus frequency.

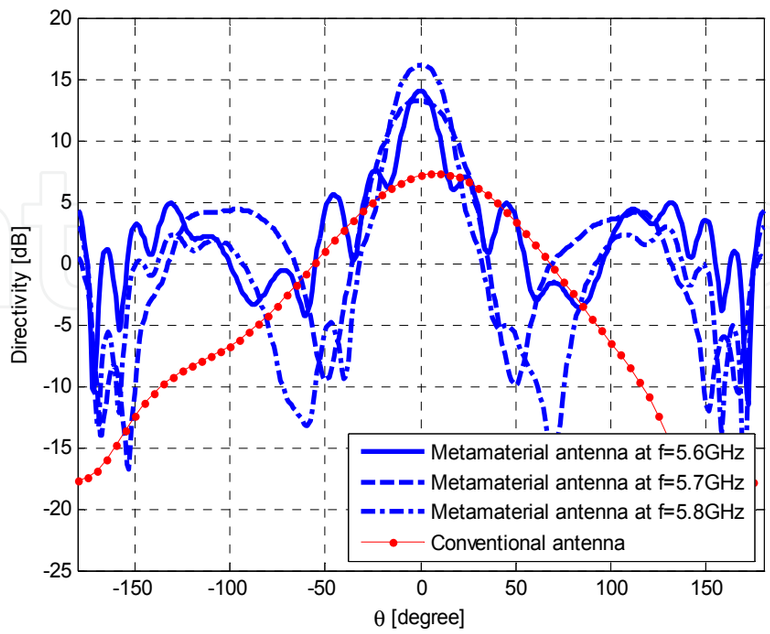

(a)

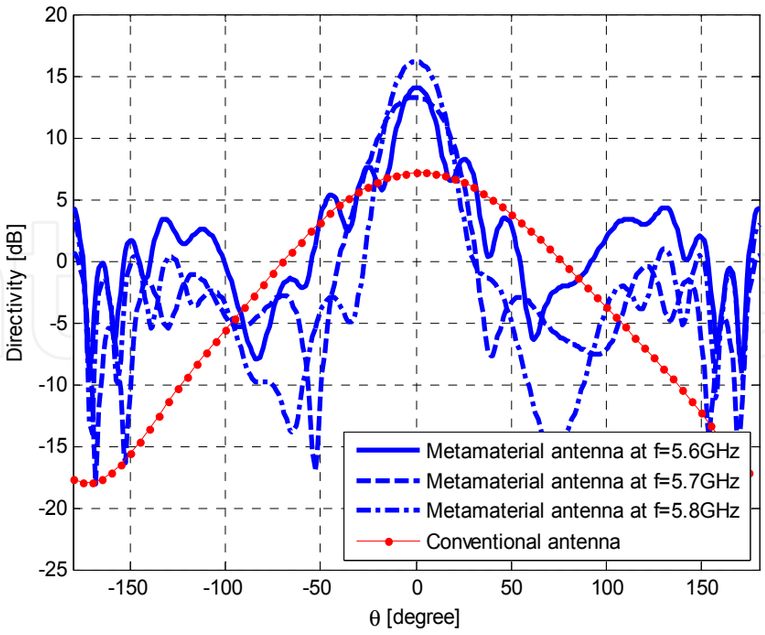

(b)

Fig. 7. CST simulated radiation patterns at different frequencies over the operating bandwidth, (a) E-plane, and (b) H-plane.

3. Polarization dependent metamaterial cover designs

A considerable part of research at microwave frequencies is focused on isotropic metamaterial covers that are independent on polarization states. Polarization-dependent surfaces have recently found useful applications in changing the polarization state of the incident wave (Yang & Rahmat-samii, 2005; Veysi et al., 2010).

For a traditional metamaterial cover, the transmission phase remains the same regardless of the *x*- or *y*-polarization state of the incident plane wave. In contrast, the transmission phase of a PDMTM cover is a function of both frequency and polarization state. Hence, when a PDMTM cover is employed as a director, the polarization state of the transmitted wave is fully characterized by the transmission phase difference between the *x*- and *y*-polarizations and the polarization state of the incident wave. And thus a proper phase difference between *x*- and *y*-polarized waves leads to a desired change in the polarization state of the transmitted wave.

Directive circularly polarized antennas are widely used in satellite communication systems. To obtain directive circularly polarized antenna, various types of metamaterial antenna have been proposed in the literature (Iriarte et al., 2006; Diblanc et al., 2005; Arnaud et al., 2007). It was demonstrated in (Iriarte et al., 2006) that the directive circularly polarized antenna can be realized by metamaterial antenna with a circular feed. A major limitation of this method is inability to tune mechanically. In other words, the polarization state of the antenna is only determined by the feed mechanism.

Directive circularly polarized antenna can be also realized using either metallic wire polarizer (Diblanc et al., 2005) or meander line polarizer (Arnaud et al., 2007) stacked on the

top of the one-layer metamaterial cover. In this section, instead of using meander line or metallic wire polarizer, the geometry of the metamaterial cover is changed to provide circular polarization. Consequently, the second layer (polarizer layer) can be replaced with another metamaterial cover layer, which in turn results in higher directivity.

Moreover, in contrast to the previous directive circularly polarized antennas (Iriarte et al., 2006; Diblanc et al., 2005; Arnaud et al., 2007), polarization state of the directive antennas using our proposed metamaterial cover can be mechanically changed regardless of the feed mechanism.

In this section, a useful guideline has been established as how to use the magnitude and phase of the transmission coefficient to identify the operational frequency band of the directive circularly polarized antennas based on polarization dependent metamaterial covers.

As revealed in the previous sections, when a plane wave normally impinges upon a metamaterial cover, the phase and magnitude of the transmitted wave change with frequency. In order to illustrate the polarization feature of the PDMTM cover, we assume that a left-hand circularly polarized (LHCP) wave, namely,

$$\vec{E^i} = \vec{a}_x e^{-jkz} + j\vec{a}_y e^{-jkz}$$

where k is the free-space wavenumber, is normally impinged upon a director placed in X-Y plane. The field transmitted through the director can be easily calculated from the following equation:

$$\vec{E^t} = e^{-jkz} e^{j\theta_x} (\vec{a}_x + j\vec{a}_y e^{j(\theta_y - \theta_x)}) \tag{5}$$

The above field can be decomposed into two circularly polarized components

$$\vec{E^t} = e^{-jkz} e^{j\theta x} [\vec{e}_r (\frac{1 - e^{j(\theta y - \theta x)}}{\sqrt{2}}) + \vec{e}_l (\frac{1 + e^{j(\theta y - \theta x)}}{\sqrt{2}})] \tag{6}$$

Where

$$\vec{e}_l = \frac{(\vec{a}_x + j\vec{a}_y)}{\sqrt{2}}, \quad \vec{e}_r = \frac{(\vec{a}_x - j\vec{a}_y)}{\sqrt{2}}$$

and θ_x and θ_y denote the transmission phases for the x- and y-polarized waves, respectively. For a traditional metamaterial cover (θ_y- θ_x=0), the transmitted wave is purely LHCP and thus the polarization does not change. In order to change the polarization state of the antenna, the PDMTM cover can be used as a director. At a certain frequency where phase difference is 180° and transmission is considerable, the transmitted wave is purely right-hand circularly polarized (RHCP).

The left-hand circularly polarized incident wave can be also converted to the linearly polarized (LP) wave where the phase difference is 90° and the transmission is also considerable. One can follow the same procedure for the linearly polarized incident wave,

$$\vec{E^i} = \vec{a}_x e^{-jkz} + \vec{a}_y e^{-jkz},$$

so that the transmitted field then becomes:

$$\vec{E^t} = \vec{a_x} e^{-j(kz-\theta x)} + \vec{a_y} e^{-j(kz-\theta y)} = e^{-jkz} e^{j\theta x} [\vec{e_r} (\frac{1+e^{j(\theta y-\theta x+\pi/2)}}{\sqrt{2}}) + \vec{e_l} (\frac{1-e^{j(\theta y-\theta x+\pi/2)}}{\sqrt{2}})] \quad (7)$$

Consequently the radiation mechanism of the linearly polarized antenna with metamaterial cover is conceptually described by Eq. 7. For an isotropic metamaterial cover, the phase difference between two orthogonal polarizations is zero and thus the polarization state does not change.

An interesting feature of the PDMTM covers can be revealed by a closer investigation. When a PDMTM cover with 90° transmission phase difference is used as a director, the polarization state of the transmitted wave becomes LHCP. Moreover, when the phase difference is -90° the polarization state of the transmitted wave is RHCP. Consequently we can easily switch between LHCP and RHCP using a rotatory cover, which can be rotated smoothly with a 90° steps.

Based on above discussion, one can conclude that the metamaterial cover can be used as a changing polarization plane. The operational frequency band of an antenna with PDMTM cover is defined as the frequency region within which the magnitudes of the transmission coefficients for both *x*- and *y*-polarized waves are close to their maximum values and transmission phase difference takes the desired value.

This interesting feature has been realized by changing the unit cell geometry, such as cutting rectangular holes instead of square holes and changing the relative height difference between the *x*- and *y*-directed strips of each layer (Veysi et al., 2011).

3.1 Rectangular hole metamaterial cover

The traditional metamaterial cover uses symmetric square holes so that its transmission phase for normal incidence remains the same regardless of the *x*- or *y*-polarization state of the incident plane wave. Therefore, the logical step is to replace the square holes by rectangular ones (Veysi et al., 2011).

First, the design parameters of the metamaterial cover are selected to have a reasonable transmission at a specified frequency. The effect of different design parameters of the metamaterial cover on the magnitude of the transmission coefficient can be found in (Huang et al., 2009).

After the successful design of the isotropic metamaterial cover, the width or/and length of the square holes are changed to obtain both the desired transmission phase difference and the maximum transmission within the specified frequency band. When the hole width is increased, the plasma frequencies shift down to the lower frequencies.

Thus, by adjusting the width and length of the rectangular hole, the polarization sense of the transmitted wave can be changed. An example design for these parameters is as follows:

h= 24.5mm, P=20.5mm, L=17.5mm, W=16.5mm

For a linearly polarized antenna, namely

$$\vec{E^i} = \vec{a_x} e^{-jkz} + \vec{a_y} e^{-jkz},$$

The axial ratio of the transmitted wave is plotted in Fig. 8. Also, Fig. 9 shows the transmission curve for both *x*- and *y*-polarized incident plane waves. The frequency band inside which the axial ratio of the RHCP transmitted wave is below 6dB and the magnitudes of the transmission coefficients for both the *x*- and *y*-polarized incident waves are more than 90% ranges from 4.75GHz to 5GHz (5.12%).

3.2 Metamaterial cover with nonplanar strips

Another approach to realize PDMTM covers is to add space between the *x*- and *y*-directed strips of each layer (Veysi et al., 2011), as shown in Fig. 10. For a traditional metamaterial cover, the *x*-directed strip is located on the same plane as the y-directed strip.

For the nonplanar case discussed here the dimensions are chosen as follows: L=W=13.5mm, P=18.5mm, h=27.5mm, h_{r1}=3.5mm, and h_{r2}=7mm, where h_{r1} denotes the relative height between the *x*- and *y*-directed strips of the first layer and h_{r2} denotes the same height for the second layer.

Fig. 11 shows the magnitudes of the transmission coefficients for both *x*- and *y*-polarized waves. The axial ratio of the wave radiated from linearly polarized antenna is also plotted in Fig. 12. It can be seen from Figs. 11-12, that the operating frequency of the proposed structure is around 9.1GHz where the metamaterial cover has both the desired transmission phase difference and the remarkable transmission.

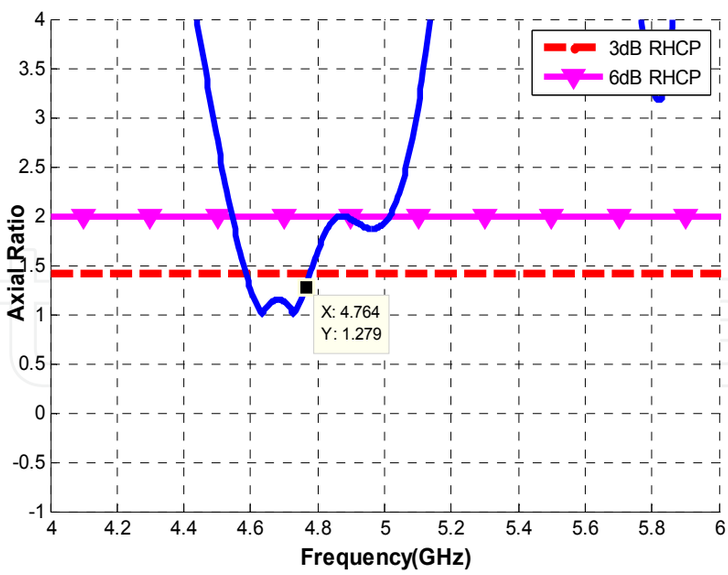

Fig. 8. Axial ratio of the transmitted plane wave from the rectangular hole metamaterial cover (Veysi et al., 2011).

The FDTD simulated results presented in this section confirm the concepts of the proposed approach to control both the direction and the polarization of the transmitted wave. The

authors believe that the proposed cover can find many applications in the broad electromagnetic areas such as antenna engineering and optical sources.

However, a rigorous characterization should take into account the complex interactions between the antenna and the metamaterial cover, such as finite size of the ground plane and the antenna height. Consequently, it is indispensable to use full wave analysis method, such as the finite difference time domain (FDTD), in the antenna designs in order to obtain accurate results.

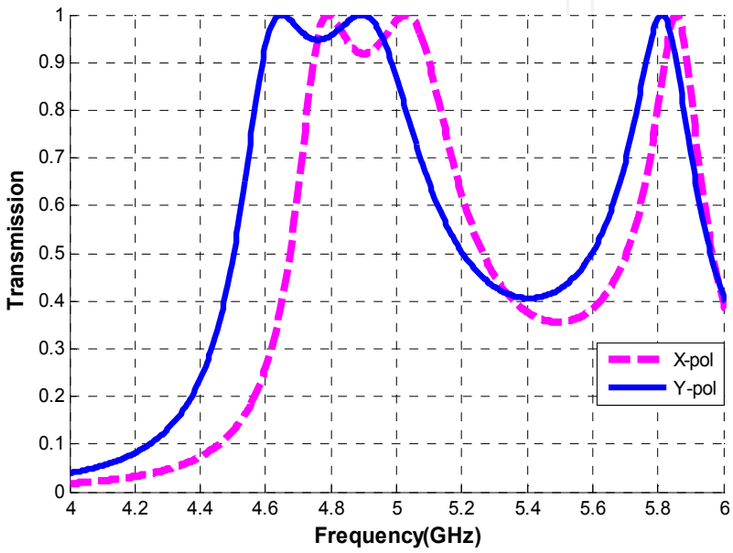

Fig. 9. FDTD simulated transmission of the rectangular hole metamaterial cover (Veysi et al., 2011).

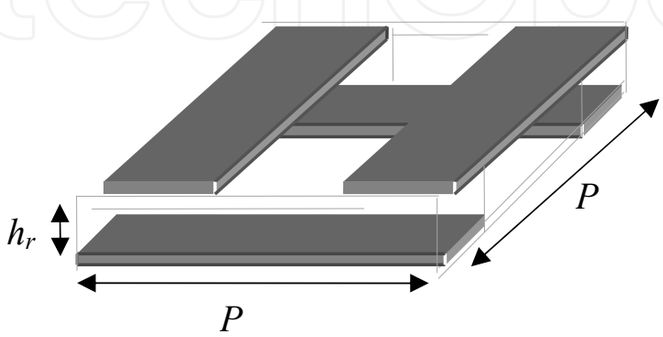

Fig. 10. A unit cell of metamaterial cover with offset strips (Veysi et al., 2011).

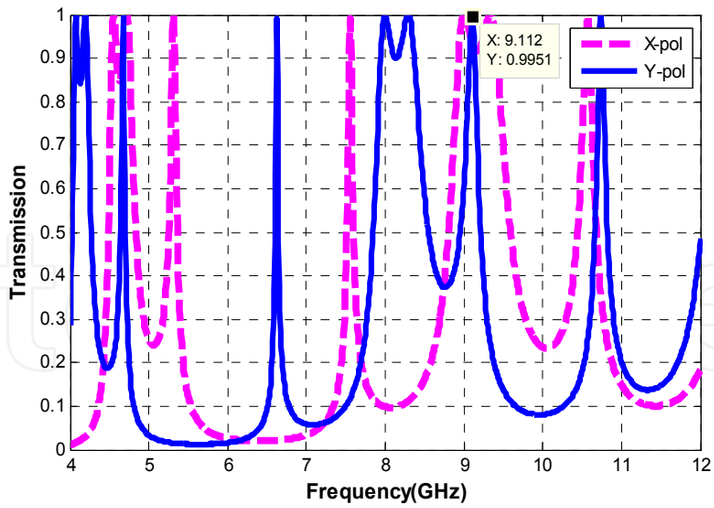

Fig. 11. FDTD simulated transmission of the metamaterial cover with offset strips (Veysi et al., 2011).

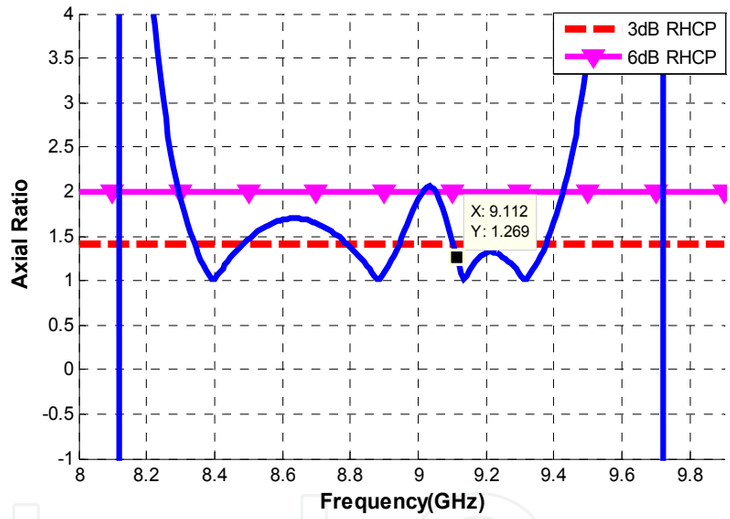

Fig. 12. Axial ratio of the transmitted plane wave from the metamaterial cover with nonplanar strips (Veysi et al., 2011).

4. Conclusions

Metamaterial covers can be applied to conventional antenna to improve their performance. These include conventional metamaterial covers to increase both the impedance and directivity bandwidths of the proximity coupled microstrip patch antenna and polarization dependent metamaterial covers to change the polarization state of the antenna. Thin lattices of ungrounded metal plates can behave as a metamaterial cover and can be analyzed using a simple FDTD code. These surfaces have two important properties: (1) increasing of the transmission rate and (2) control of the direction and polarization of the transmission. Polarization dependent metamaterial covers can be realized by cutting rectangular holes instead of square holes and changing the relative height difference between the *x*- and *y*-directed strips of each layer.

5. References

Alù, A., Bilotti, F., Engheta, N. & Vegni, L. (2006). Metamaterial Covers Over a Small Aperture, *IEEE Trans. Antennas Propag*., Vol. 54, No. 6, pp. 1632–1643

Arnaud, E., Chantalat, R., Koubeissi, M., Menudier, C., Monediere, T., Thevenot, M., & Jecko, B. (2007). New Process of Circularly Polarized EBG Antenna by using meander Lines, *IET, EuCAP*, pp. 1-6

Diblanc, M., Rodes, E., Amaud, E., Thevenot, M., Monediere, T., & Jecko, B. (2005). Circularly Polarized Metallic EBG Antenna, *IEEE Microwave and Wireless Components Letters*., Vol. 15, No. 10, pp. 638-640

Enoch, S., Tayeb, G., Sabouroux, P., Guérin, N., & Vincent, P. (2002). A Metamaterial for Directive Emission, *Physical Review Letters*, Vol. 89, pp. 213902

Garg, R., Bhartia, P., Bahl, I., Ittipiboon, A. (2001). Microstrip Antenna Design Handbook, *Artech House*

Huang, C., Zhao, Z., Wang, W., & Luo, X. (2009). Dual Band Dual Polarization Directive Patch AntennaUsing Rectangular Metallic Grids Metamaterial, *Int J Infrared Milli Waves*, Vol. 30, pp. 700–708

Iriarte, J. C., Ederra, I., Gonzalo, R., Gosh, A., Laurin, J., Caloz, C., Brand, Y., Gavrilovic, M., & Demers, Y. P. (2006). EBG Superstrate for Gain Enhancement of a Circularly Polarized Patch Antenna", *IEEE Trans. Antennas Propag*., pp. 2993-2996

Jafargholi A, Kamyab, M., Veysi, M. & Nikfal Azar, M. (2011), Microstrip gap proximity fed-patch antennas, analysis, and design, *Int J Electron Commun* (AEÜ), doi:10.1016/j.aeue.2011.05.011

Ju, J., Kim, D., Lee, W. J., & Choi, J. I. (2009). Wideband High-Gain Antenna Using Metamaterial Superstrate with the Zero Refractive Index, *Microwave and Optical Tech. Lett*., Vol. 51, No. 8, pp. 1973–1976

Pendry, J. B., Holden, A. J., Stewart, W. J., & Youngs, I. (1996). Extremely Low Frequency Plasmas in Metallic Mesostructures, *Physical Review Letters*, Vol. 76, pp.4773-4776

Temelkuaran, B., Bayindir, Ozbay, M., E., Biswas, R., Sigalas, M., Tuttle, G., & Ho, K. M. (2000). Photonic Crystal-Based Resonant Antenna with a Very High Directivity, *Journal of Applied Physics,* Vol. 87, pp. 603–605

Tsao, C. H. & Chen, J. L. (2006). Field Propagation of a Metallic Grid Slab That Act as a Metamaterial, *Physics Letters A*, Vol. 353, pp. 171–178

Veysi, M., Kamyab, M., Mousavi, S. M., & Jafargholi, A. (2010). Wideband Miniaturized Polarization-Dependent HIS Incorporating Metamaterials, *IEEE Antennas And Wireless Propagation Letters*, Vol. 9, pp. 764-766

Veysi, M., Kamyab, M., Moghaddasi, J., & Jafargholi, A. (2011). Transmission Phase Characterizations of Metamaterial Covers for Antenna Application, *Progress In Electromagnetics Research Letters*, Vol. 21, pp. 49-57

Xu, H., Zhao, Z., Lv, Y., Du, C., & Luo, X. (2008). Metamaterial Superstrate and Electromagnetic Band-Gap Substrate for High Directive Antenna, *Int J Infrared Milli Waves*, Vol. 29, pp. 493–498

Yang, F. & Rahmat-Samii, Y. (2005). A low profile single dipole antenna radiating circularly polarized waves, *IEEE Trans. Antennas Propag*., Vol. 53, No. 9, pp. 3083–3086

Zhong, S.-S., Liu, G. & Qasim, G. (1994). Closed Form Expressions for Resonant Frequency of Rectangular Patch Antennas With Multidielectric Layers, *IEEE Trans. Antennas Propag*., Vol. 42, pp.1360-1363

Zhu, F., Lin, Q., & Hu, J. (2005). A Directive Patch Antenna with a Metamaterial Cover, *Proceedings of Asia Pacific Microwave Conference*

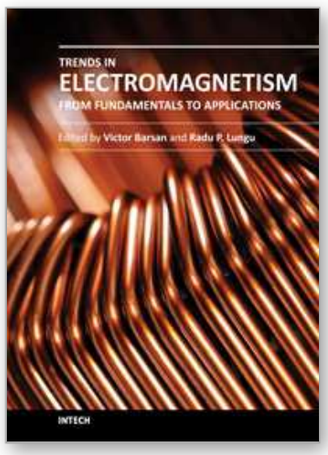

Trends in Electromagnetism - From Fundamentals to Applications

Edited by Dr. Victor Barsan

ISBN 978-953-51-0267-0

Hard cover, 290 pages

Publisher InTech

Published online 23, March, 2012

Published in print edition March, 2012

Among the branches of classical physics, electromagnetism is the domain which experiences the most spectacular development, both in its fundamental and practical aspects. The quantum corrections which generate non-linear terms of the standard Maxwell equations, their specific form in curved spaces, whose predictions can be confronted with the cosmic polarization rotation, or the topological model of electromagnetism, constructed with electromagnetic knots, are significant examples of recent theoretical developments. The similarities of the Sturm-Liouville problems in electromagnetism and quantum mechanics make possible deep analogies between the wave propagation in waveguides, ballistic electron movement in mesoscopic conductors and light propagation on optical fibers, facilitating a better understanding of these topics and fostering the transfer of techniques and results from one domain to another. Industrial applications, like magnetic refrigeration at room temperature or use of metamaterials for antenna couplers and covers, are of utmost practical interest. So, this book offers an interesting and useful reading for a broad category of specialists.

How to reference

In order to correctly reference this scholarly work, feel free to copy and paste the following:

Mehdi Veysi, Amir Jafargholi and Manouchehr Kamyab (2012). Theory and Applications of Metamaterial Covers, Trends in Electromagnetism - From Fundamentals to Applications, Dr. Victor Barsan (Ed.), ISBN: 978-953-51-0267-0, InTech, Available from: http://www.intechopen.com/books/trends-in-electromagnetism-from-fundamentals-to-applications/theory-and-applications-of-metamaterial-covers

INTECH
open science | open minds

InTech Europe
University Campus STeP Ri
Slavka Krautzeka 83/A
51000 Rijeka, Croatia
Phone: +385 (51) 770 447
Fax: +385 (51) 686 166
www.intechopen.com

InTech China
Unit 405, Office Block, Hotel Equatorial Shanghai
No.65, Yan An Road (West), Shanghai, 200040, China
中国上海市延安西路65号上海国际贵都大饭店办公楼405单元
Phone: +86-21-62489820
Fax: +86-21-62489821

IntechOpen